

SUPPLEMENT FILE 6

Based on along-strike variations in geometry, kinematics and the presence of slip partitioning, the surface rupture in the Sierra domain was divided into six segments and these subdivided into 49 sections, which have an average length of ~1.0 km (Table SF6-1 and Figs. SF6-1 to SF6-3). Note that these short sections are defined as a basis for organizing the fault measurement data, and do not correspond to rupture segments as commonly used for seismic hazard estimation.

In Table SF6-1, we report the orientation and kinematics of each fault section determined from the main datasets presented in this study. For fault section orientations, section strike was determined from the trend of the line connecting the rupture section endpoints, and dip was calculated using Bingham statistics for the rupture sections with multiple measurements of master fault orientation. In general, scarp-forming fractures are oriented at higher dip angles than the master fault along which they propagated. Thus in sections that had no direct measurements of master fault orientation, we report the dip of the shallowest-dipping, scarp-forming fault determined using three-point solutions. Dips determined from these two methods are plotted for each section in Figures SF6-1 to SF6-3. For sections that had neither master fault nor scarp orientation data, we report the dip determined using one of the following conventions: 1) interpolated from the closest measurements found in adjacent fault sections, 2) extrapolated dip from the nearest rupture section, or 3) assumed rupture section dip based on structural context and known along-strike characteristics of the fault zone. The method for determining rupture section dip is marked in the “Dip Source” field in Table SF6-1. The average vertical and lateral slip components of each section was calculated by dividing the area of the smoothed slip

envelope by the section length. Heave was calculated using the rupture section dip and the net vertical displacement averaged over each section. Total slip is the vector sum of heave, lateral and vertical components of slip. Finally, fault section kinematics were derived using fault section orientations and the lateral and heave components of slip.

Laguna Salada Segment

Within the Laguna Salada segment, we defined six sections based on changes in kinematics and geometry (Fig. SF6-1). Sections 1 and 2 form the southern tine of the prominent splay observed near the edge of the Delta domain with minor northeast-down vertical displacements (Fig. SF6-1). The northern tine is divided in three different splays (sections 3–5) based on left-stepping discontinuities in the surface trace of the rupture, each of which also accommodated minor northeast-down vertical displacements. Section 6 is marked by a change in polarity of vertical slip to the southwest and extends to the intersection with the Pescadores fault. Dips reported in Table SF6-1 for sections 1 and 2 were determined using three-point solutions of scarp-forming faults. For sections 3–6, rupture section dip reported is based on the assumption that the Laguna Salada fault has a subvertical inclination within this segment.

Pescadores Segment

The Pescadores rupture segment shows very little along-strike variations in both orientation and kinematics, however, we identified six sections based on subtle changes in strike as well as changes in distribution of antithetic southwest-side down vertical slip (Fig. SF6-1). All rupture sections within the Pescadores segment dip $>65^\circ$ towards the northeast. For most fault sections, with the exception of section 11, dips reported in Table SF6-1 were determined from measurements of scarp-forming faults and/or master faults.

For section 11, we report the dip interpolated from the nearest measurements found in sections 10 and 12.

Puerta Accommodation Zone

EMC rupture through the Puerta accommodation zone was broadly distributed along multiple faults, including several unnamed faults and the Cascabel and Borrego faults (Fig. SF6-2). Due to the paucity of kinematic measurements in the field and the complex distribution of surface rupture between the Pescadores rupture segment and the Cascabel fault, we only recognize one section (section 13; Fig. SF6-2). This section is located ~6 km from the northern limit of the Pescadores rupture segment, dips $\sim 72^\circ$ and contains a single kinematic transect measurement (Fig. SF6-2). Along the northern portion of the accommodation zone coseismic slip is distributed between the closely spaced and subparallel Cascabel and Borrego faults, an additional four fault sections were identified based on along-strike changes in fault orientation (sections 14 to 17; Fig. SF6-2). A single section was defined along the Cascabel fault due to its relatively straight surface trace and uniformly steep inclination, whereas, along the adjacent Borrego fault, three fault sections were recognized based on $>15^\circ$ changes in strike along its length.

Borrego Segment

The Borrego rupture segment is divided into three kinematic sections (sections 18–20) defined by changes in strike (Fig. SF6-2 and Table SF6-1). These sections show systematic differences in the ratio of lateral to vertical slip measured across the scarp array. Dextral slip is maximized on section 19, which has the most westerly strike, and is minimized on section 20, which has a NNE strike and accommodates a strong sinistral component of slip (Fig. SF6-2 and Table SF6-1). Dips reported in Table SF6-1 were

determined using the shallowest dipping scarp-forming faults within each section, which commonly had moderate inclinations. Due to the moderate inclinations of these fault sections, the heave component derived for these section are an order of magnitude greater than those derived for all fault sections to the south.

Paso Inferior Accommodation Zone

The Paso Inferior accommodation zone contains the northernmost Borrego fault, an east-dipping detachment and two west-dipping faults, from which we identified 13 sections mostly based on changes in strike as well as discontinuities in the rupture trace defined by stepovers (Fig. SF6-3). The northernmost west-dipping fault was defined as a single section (section 38) due to its relatively short length.

Paso Superior Segment

The Paso Superior rupture segment is divided into 11 kinematic sections defined by changes in either fault strike (sections 39–45), a left-stepping transfer zone (section 46) or at large changes in dip due to the ramp–flat transitions of the Paso Superior detachment (sections 47–49). For sections that dip $<45^\circ$ and that accommodated significant amounts of vertical displacement, the heave component of the total coseismic slip vector is generally much greater than the vertical and lateral slip components (Table SF6-1). Section 48 represents the northernmost fault ramp where the Paso Superior detachment dips $\sim 55^\circ$, and is where the largest amount of dextral coseismic slip was measured in the Paso Superior segment.

TABLES

Table SF6-1. Table containing geometry and EMC rupture kinematics determined for the 49 fault sections identified in the Sierra domain of the EMC rupture. Longitude and latitude mark midpoint locations to fault sections.

FIGURE CAPTIONS

Figure SF6-1. Geologic map of the southern Sierra Cucapah showing schematic rupture traces (yellow lines), and the fault section boundaries and labels, geometry (ball and bar symbols) and EMC rupture kinematics (shaded envelopes). Fault section dip values are only shown for sections containing measurements of master fault plane and/or scarp-forming faults. See Figure 11 for additional information.

Figure SF6-2. Geologic map of the central Sierra Cucapah showing schematic rupture traces (yellow lines), and the fault section boundaries and labels, geometry (ball and bar symbols) and EMC rupture kinematics (shaded envelopes). Fault section dip values are only shown for sections containing measurements of master fault plane and/or scarp-forming faults. See Figure 14 for additional information.

Figure SF6-3. Geologic map of the northern Sierra Cucapah showing schematic rupture traces (yellow lines), and the fault section boundaries and labels, geometry (ball and bar symbols) and EMC rupture kinematics (shaded envelopes). Fault section dip values are only shown for sections containing measurements of master fault plane and/or scarp-forming faults. See Figure 18 for additional information.

Table SF6-1. Table of fault section geometry and EMC rupture kinematics.

Longitude	Latitude	Length (m)	Domain	Segment	Fault	Section	Strike	Dip	Dip Source	Lateral (cm)	Vertical (cm)	Heave (cm)	Total (cm)	Slip Azimuth	Slip Plunge	Slip Rate	Max. Instant. Extension Azimuth
-115.336473	32.271493	1981	Sierra	Laguna Salada	LS south line	1	314	81	scarp	21	3	0	21	133	8	172	269
-115.346684	32.281777	1167	Sierra	Laguna Salada	LS south line	2	326	73	scarp	45	28	9	54	135	31	147	93
-115.331692	32.283651	1262	Sierra	Laguna Salada	LS north line	3	306	85	assumed ¹	54	3	0	54	126	3	177	261
-115.341333	32.287809	1862	Sierra	Laguna Salada	LS north line	4	295	85	assumed ¹	19	20	2	28	110	47	133	58
-115.353071	32.288910	842	Sierra	Laguna Salada	Laguna Salada	5	291	85	assumed ¹	128	18	2	129	110	8	172	65
-115.374864	32.299136	2845	Sierra	Laguna Salada	Laguna Salada	6	122	85	assumed ¹	128	31	3	132	301	14	166	256
-115.393149	32.309883	1370	Sierra	Pescadores	Pescadores	7	307	85	fault	101	30	3	105	125	17	163	80
-115.404150	32.317806	1392	Sierra	Pescadores	Pescadores	8	302	75	scarp	185	42	11	190	119	13	167	256
-115.432191	32.338476	5668	Sierra	Pescadores	Pescadores	9	315	76	scarp	189	82	20	207	129	23	156	86
-115.457978	32.361010	1321	Sierra	Pescadores	Pescadores	10	310	74	scarp	276	69	20	285	126	14	165	263
-115.467630	32.369443	1301	Sierra	Pescadores	Pescadores	11	324	75	assumed ²	239	66	18	249	140	15	164	277
-115.486009	32.386726	3926	Sierra	Pescadores	Pescadores	12	310	68	scarp	235	79	32	250	122	18	160	261
-115.567290	32.436601	826	Sierra	Puerta	Unnamed Fault	13	335	72	fault	57	91	30	111	128	55	121	88
-115.589833	32.449393	3279	Sierra	Puerta	Cascabel	14	321	77	fault	144	79	18	165	134	28	151	90
-115.597439	32.448969	1340	Sierra	Puerta	Borrego	15	324	62	scarp	0	69	37	78	54	62	90	54
-115.601844	32.455587	361	Sierra	Puerta	Borrego	16	341	56	scarp	0	65	44	78	71	56	90	71
-115.603980	32.459057	544	Sierra	Puerta	Borrego	17	322	69	scarp	33	30	12	46	123	40	136	84
-115.610448	32.462125	1324	Sierra	Borrego	Borrego	18	330	41	scarp	74	153	177	245	83	39	108	252
-115.618268	32.470909	1236	Sierra	Borrego	Borrego	19	317	40	scarp	157	151	179	282	88	32	124	250
-115.621902	32.478259	704	Sierra	Borrego	Borrego	20	15	47	scarp	47	127	118	180	84	45	75	95
-115.622446	32.484217	709	Sierra	Paso Inferior	Borrego	21	335	84	scarp	190	96	10	213	152	27	153	106
-115.628565	32.490841	1238	Sierra	Paso Inferior	Borrego	22	316	80	fault	254	117	21	280	131	25	155	86
-115.635238	32.497748	762	Sierra	Paso Inferior	Borrego	23	333	75	assumed ³	54	47	13	73	140	40	138	96
-115.636988	32.506186	1159	Sierra	Paso Inferior	Borrego	24	355	75	assumed ³	158	46	12	165	170	16	163	127
-115.636122	32.485068	615	Sierra	Paso Inferior	Unnamed Detachment	25	298	45	fault	78	3	3	78	116	2	177	261
-115.641037	32.487893	517	Sierra	Paso Inferior	Unnamed Detachment	26	317	45	assumed ³	61	1	1	61	136	1	179	281
-115.645260	32.490874	554	Sierra	Paso Inferior	Unnamed Detachment	27	304	45	assumed ³	146	31	31	152	112	12	163	260
-115.650294	32.492119	317	Sierra	Paso Inferior	Unnamed Detachment	28	329	45	assumed ³	54	41	41	79	112	31	133	268
-115.651226	32.495353	412	Sierra	Paso Inferior	Unnamed Detachment	29	331	45	assumed ³	5	33	33	47	69	45	96	65
-115.655500	32.497793	447	Sierra	Paso Inferior	Unnamed Detachment	30	328	45	assumed ³	22	35	35	54	90	40	114	254
-115.656747	32.502921	727	Sierra	Paso Inferior	Unnamed Detachment	31	347	45	assumed ³	3	19	9	21	95	64	98	83
-115.649023	32.503125	433	Sierra	Paso Inferior	Unnamed Fault	32	164	65	assumed ³	2	30	14	33	261	65	93	256
-115.649853	32.507630	590	Sierra	Paso Inferior	Unnamed Fault	33	178	65	assumed ³	0	77	36	85	268	65	90	268
-115.651158	32.512993	654	Sierra	Paso Inferior	Unnamed Fault	34	153	65	assumed ³	0	104	49	115	243	65	90	243
-115.656136	32.517521	751	Sierra	Paso Inferior	Unnamed Fault	35	131	65	assumed ³	4	37	17	41	235	64	96	226
-115.659594	32.523341	779	Sierra	Paso Inferior	Unnamed Fault	36	170	58	scarp	0	54	34	64	260	58	90	260
-115.661837	32.530938	971	Sierra	Paso Inferior	Unnamed Fault	37	161	62	scarp	4	13	7	15	281	59	105	262
-115.670105	32.524291	1568	Sierra	Paso Inferior	Unnamed Fault	38	168	65	assumed ³	6	54	25	60	272	64	96	263
-115.684467	32.534098	654	Sierra	Paso Superior	Paso Superior	39	342	40	assumed ³	87	125	149	213	102	36	114	269
-115.687301	32.538049	407	Sierra	Paso Superior	Paso Superior	40	333	40	assumed ³	29	93	111	148	77	39	101	251
-115.689159	32.543011	770	Sierra	Paso Superior	Paso Superior	41	336	38	scarp	22	203	260	331	71	38	94	249
-115.691132	32.547321	261	Sierra	Paso Superior	Paso Superior	42	351	37	scarp	44	139	185	236	95	36	101	269
-115.694452	32.552892	1169	Sierra	Paso Superior	Paso Superior	43	324	32	fault	96	104	166	218	84	28	116	253
-115.703499	32.561761	1544	Sierra	Paso Superior	Paso Superior	44	321	35	fault	42	82	117	149	70	33	106	242
-115.713817	32.570997	1337	Sierra	Paso Superior	Paso Superior	45	313	32	fault	100	24	38	110	112	12	156	269
-115.719326	32.572418	979	Sierra	Paso Superior	Paso Superior	46	328	21	fault	76	20	51	94	114	12	144	280
-115.724374	32.580247	1002	Sierra	Paso Superior	Paso Superior	47	350	20	fault	112	80	218	258	107	18	116	279
-115.728026	32.590010	1439	Sierra	Paso Superior	Paso Superior	48	332	55	fault	165	100	70	205	129	29	144	276
-115.733230	32.597316	385	Sierra	Paso Superior	Paso Superior	49	327	37	fault	24	46	61	80	78	35	107	249

¹ Dip based on assumption that LSF is a subvertical fault.

² Dip is interpolated using nearest observations from adjacent segments

³ Dip is extrapolated using observations from nearest segments.

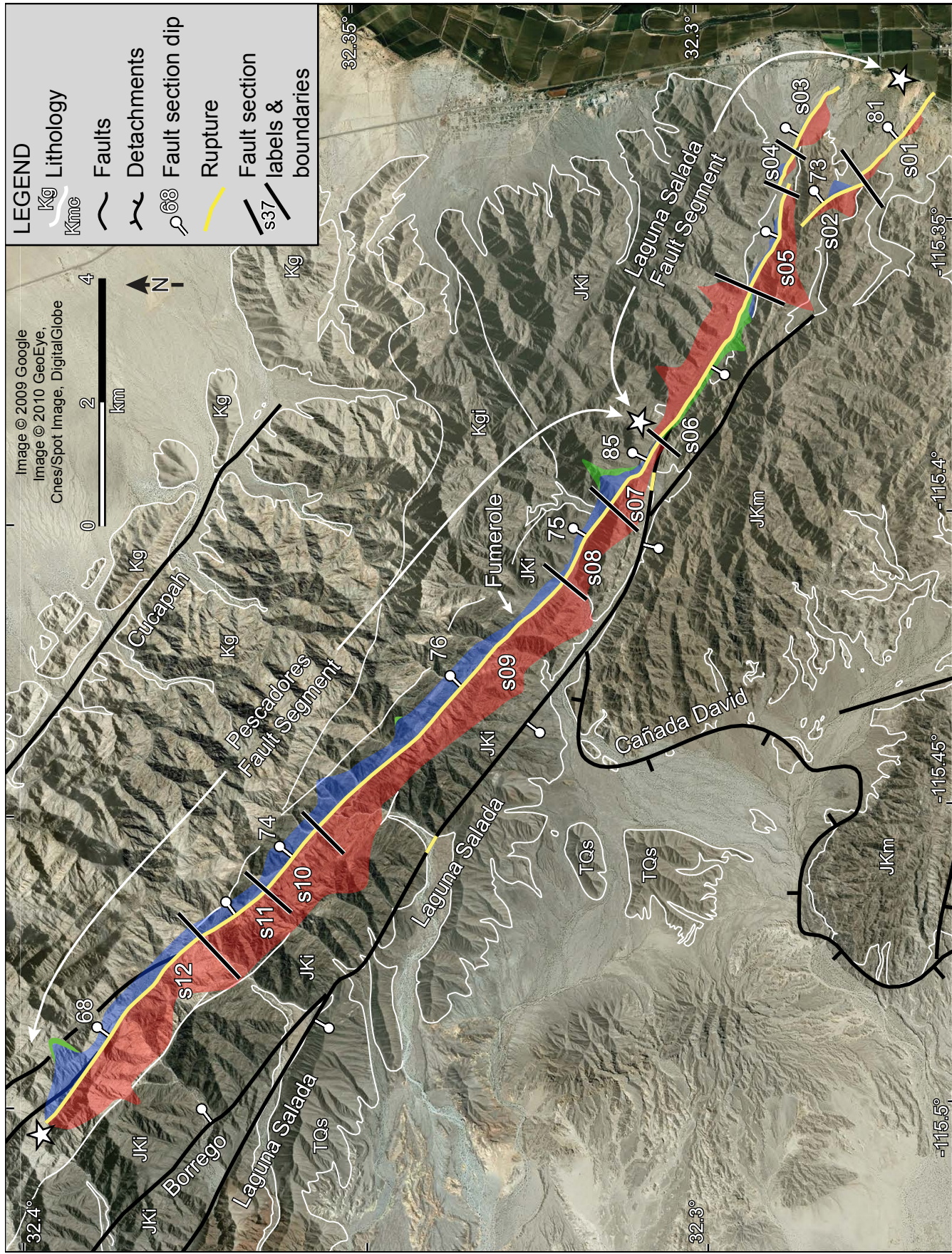


Figure SF6-1

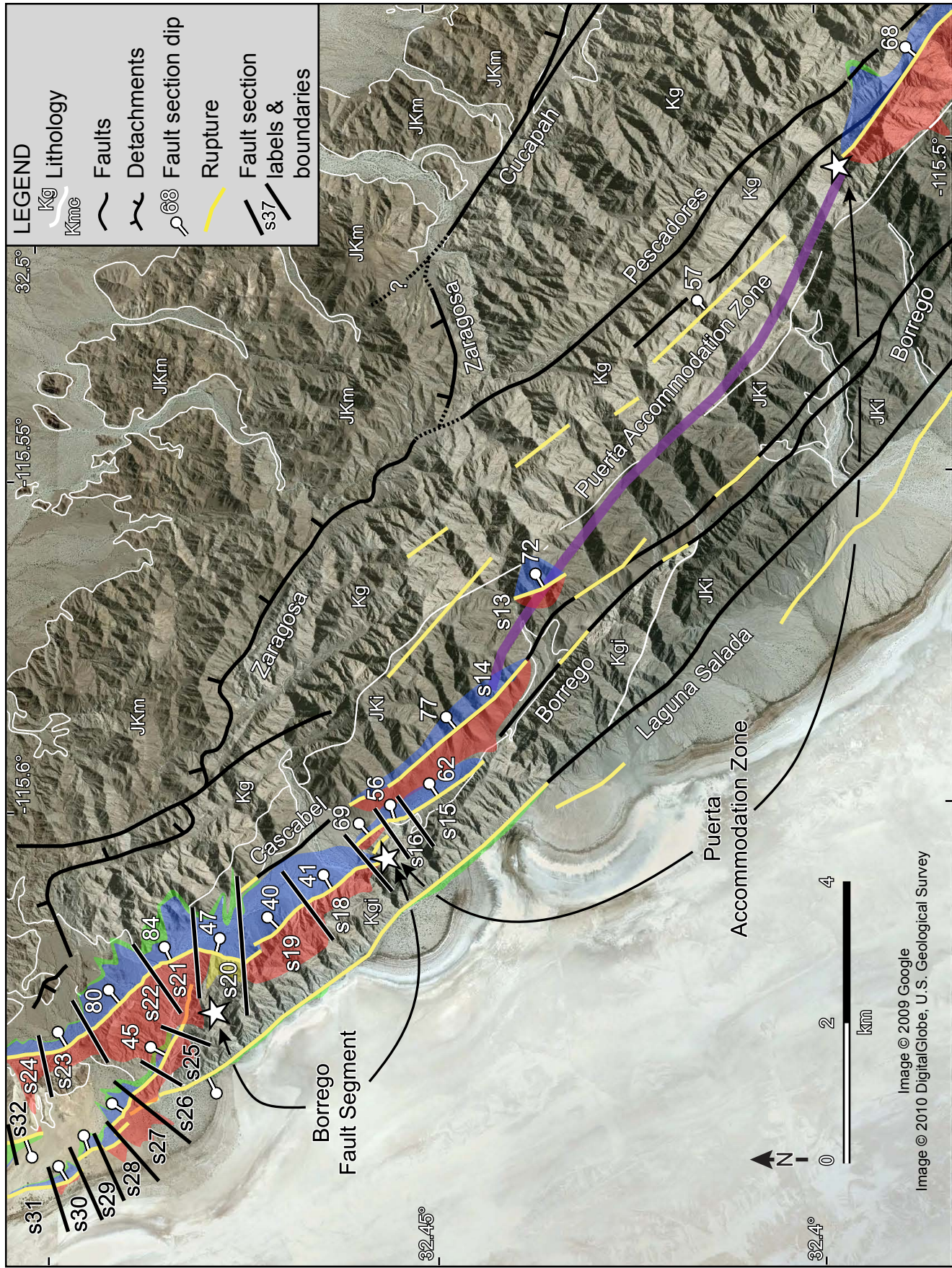


Figure SF6-2

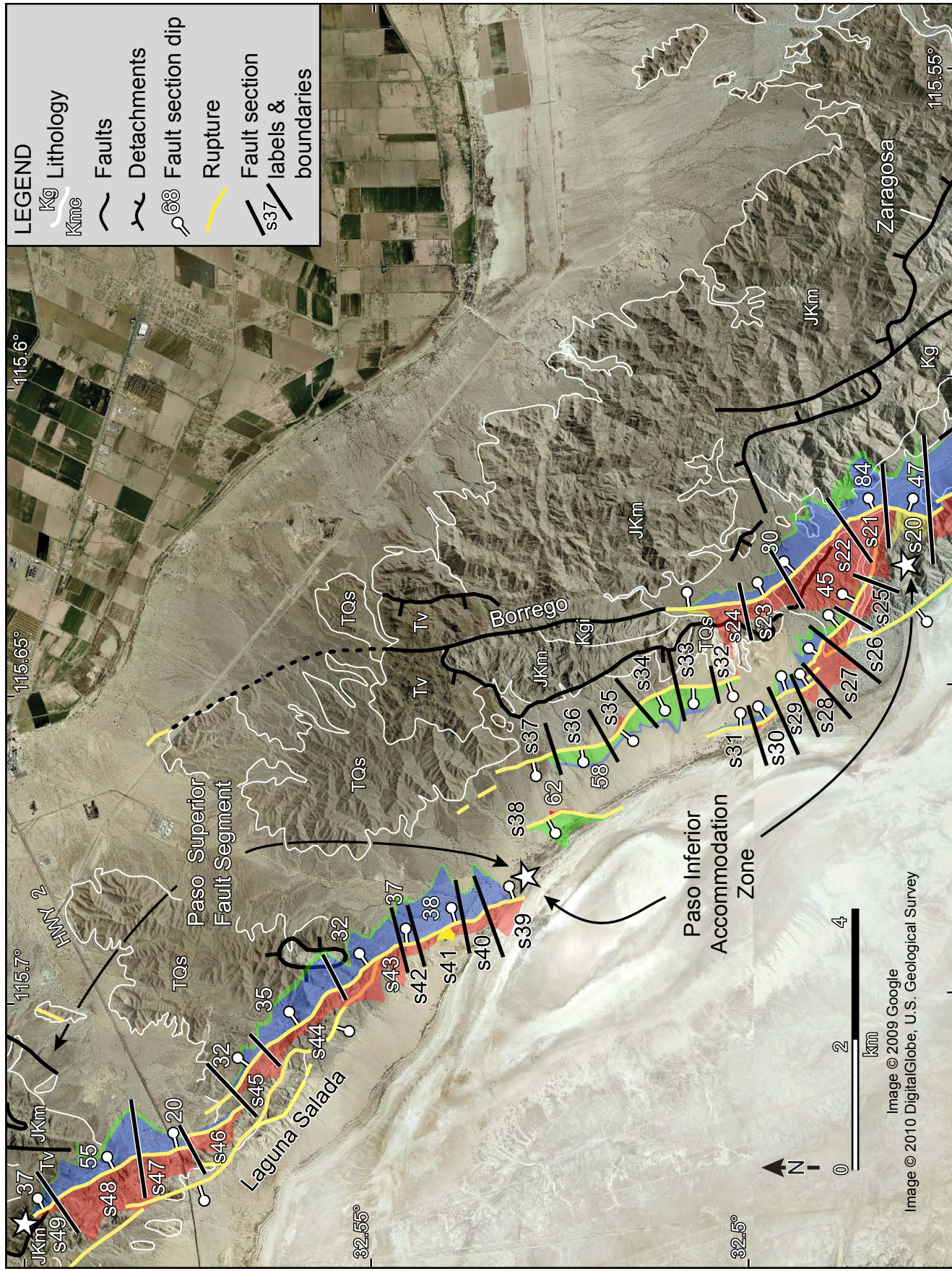


Figure SF6-3